Flexible control of grid-connected renewable energy systems inverters under unbalanced grid faults

Bassam Alhamazani [1], Rabeh Abbassi [1, *], Hani Aloufi [1], Badr Alshammari [1], Houssem Jerbi [2], Saleh Albadran [1]

[1]Department of Electrical Engineering, College of Engineering, University of Ha'il, Ha'il, Saudi Arabia
[2]Department of Industrial Engineering, College of Engineering, University of Ha'il, Ha'il, Saudi Arabia

ARTICLE INFO

ABSTRACT

The sustainable energy opportunity of the future lies in the renewable energy-based distributed Power Generation systems (DPGSs). However, there are different concerns and integration issues that surround them. To increase the rate at which renewable energy can be used, this paper focuses on an integrated utility grid system. A novel strategy to control the grid side inverter is developed for a DPGS when considering an unbalanced grid. First, an analysis of the consequences of the occurrence of a fault on the grid is performed. Secondly, a control strategy is proposed to ensure the operation of the DPGS connected to the grid even if the latter is unbalanced. The proposed approach consists in developing control loops for each of the three symmetrical sequences in a specific reference frame to ensure the operation of the grid-connected DPGS even during asymmetrical grid voltage fault. The found results are promising in terms of the guarantee of service continuity during faulty conditions.

1. Introduction

Pollution is a side effect of all the energy-associated forms, especially the conventional forms. In order to eradicate the concern of environmental pollution, sustainable energy sources have to be considered for the future of the planet. The liberalization of energy and electricity development through sustainable sources is in progress (Maisanam et al., 2021). Renewable energy is consistently increasing and paving the way for an advantage in consumer usage in the electricity market (Hassan et al., 2020). There are many sources of renewable energy through which electricity generation takes place and these have vast investments and higher penetration rates (Oliva et al., 2022). Wind energy conversion systems (WECS) (Jin et al., 2021) or Photovoltaic systems (PVS) (Aboagye et al., 2022; Hamidi et al., 2020; Abbassi et al., 2018) have seen the highest penetration rates. Wind energy and photovoltaic sources of electricity are fluctuating in nature due to the availability of sun and wind movement (Latifi et al., 2021). A

convincing solution or multiplication of different kinds is needed to make them more reliable and to reduce the unpredictability of the natural renewable source potential (Zhao et al., 2021).

The demand for the production and distribution of electricity through hybrid renewable energy systems (HRES) and technologies is increasing. Optimizing power generation systems through renewable energy sources and their combinations will be a solution to power up rural and remote areas (Abbassi et al., 2019). This would be an economic and technical solution. Apart from this, renewable energy from wind and solar can be grid-connected.

The distributed power generation system and its increased penetration made to ponder the condition of the balanced or unbalanced network condition (Li et al., 2021). The distributed power generation system should work and provide service even when there is an imbalance in the grid (Tang et al., 2021). Power electronics, in this case, would initiate a revolution in the use of HRES systems. The power electronic converters are exploited to interface the decentralized production unit with the network (Yin et al., 2021). If the DPGS power is not controlled, there could be problems faced by the consumer when they are connected to the utility grid hence there should be considerations on the safe of operation, production of electricity, etc (Mohammadinodoushan et al., 2021). In addition,

synchronization should be ensured before the system is connected to the utility grid.

The work presented here focuses on this type of application in order to have an advantageous effect on the energy production system, through cost-saving, availability, and providing a solution to the problem of renewable energy-based power systems (Bensalem et al., 2021). There are chances of instabilities and other problems that could occur when there is large-scale integration of decentralized production in the main grid.

This work is executed to optimally design a grid-connected DPGS system during faulty conditions. The impacts of the grid voltage imbalance are studied and new algorithms are investigated to solve such problems.

2. Relevant works

2.1. GSC control in balanced mode

The VSCs control has received major attention for many decades. The Direct power control (DPC) (Saidi et al., 2014), the Direct Torque Control (DTC) (Wang et al., 2020; Nasr et al., 2022), and the

Voltage-oriented control (VOC) (Zamani et al., 2015) were investigated.

With one control strategy or the other, the inverters are used with the main objective of permitting and getting the sinusoidal voltage with adjustable amplitude and fundamental frequency, through this, there will be an elimination or postponement of high-frequency harmonic parasites that result from switching (Saidi et al., 2016). This is equivalent to a filtering principle that is related to passive filtering.

To transfer power efficiently from one renewable energy system to the electrical grid, the three-phase VSC is used as a dominant topology for controlled applications. The distortion of current is decreased and the filtering requirements are done with the ability to control the DC bus voltage through the pulse width modulation operation (PWM) (Venkatesan et al., 2020). The three-phase VSCs are widely implemented for a vast series of power applications based on a trio of key elements: Such as the synchronization of the grid, the internal loop and modulation, and the external loop as referred to in Fig. 1.
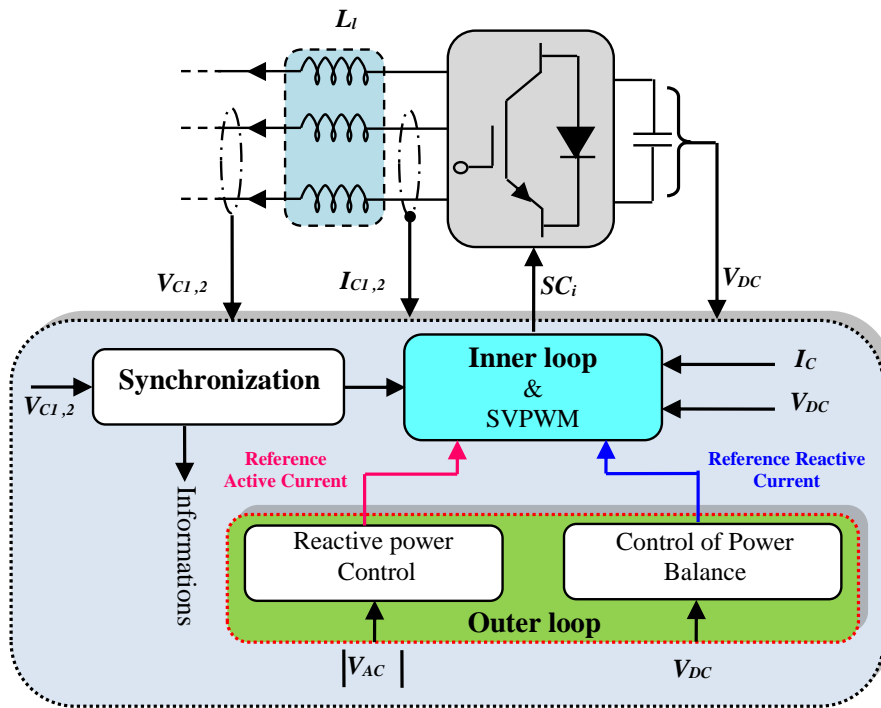

Fig. 1: Cascaded control loop of the GSC

In an aspect of advanced inverter control, Chen et al. (2016), and Mahlooji et al. (2018) proposed some innovative techniques that were considered very useful for grid-connected applications. The approach developed by Zhang et al. (2021) has been equally effective for inverter current control. In recent years, this context of study has gained great popularization due to the various applications that have been made. Particularly, voltage source converters (VSI) are most widely used in different applications (Han et al., 2016).

2.2. Effects of voltage imbalance on electric quantities

The adverse effect which is a result of the voltage imbalance in the network is the focus of interest. Generally, the methods of resolution for the unbalanced three-phase system are based on the concept of Fortescue which disintegrates it into three balanced sequences (Abbassi et al., 2019). As illustrated in Fig. 2, such sequences: The positive, the negative, and the zero sequences of the grid voltage system in its complex form (or phasor

representation) of Eq. 1 are expressed in Eqs. 2, 3, and 4 with $a = e^{j \cdot \frac{2\pi}{3}}$.

$$\begin{bmatrix} \underline{v}_{ga} \\ \underline{v}_{gb} \\ \underline{v}_{gc} \end{bmatrix} = \begin{bmatrix} V_a \{cos(\omega.t + \varphi_a) + j.sin(\omega.t + \varphi_a)\} \\ V_b \{cos(\omega.t + \varphi_b) + j.sin(\omega.t + \varphi_b)\} \\ V_c \{cos(\omega.t + \varphi_c) + j.sin(\omega.t + \varphi_c)\} \end{bmatrix} \quad (1)$$

$$\begin{bmatrix} v_{ga}^P \\ v_{gb}^P \\ v_{gc}^P \end{bmatrix} = \frac{1}{3} \begin{bmatrix} 1 & a & a^2 \\ a^2 & 1 & a \\ a & a^2 & 1 \end{bmatrix} . \begin{bmatrix} v_{ga} \\ v_{gb} \\ v_{gc} \end{bmatrix} = \begin{bmatrix} V_g^P . e^{j(\omega t + \varphi_P)} \\ V_g^P . e^{j(\omega t + \frac{2}{3}\pi + \varphi_P)} \\ V_g^P . e^{j(\omega t - \frac{2}{3}\pi + \varphi_P)} \end{bmatrix} \quad (2)$$

$$\begin{bmatrix} v_{ga}^N \\ v_{gb}^N \\ v_{gc}^N \end{bmatrix} = \frac{1}{3} \begin{bmatrix} 1 & a^2 & a \\ a & 1 & a^2 \\ a^2 & a & 1 \end{bmatrix} . \begin{bmatrix} v_{ga} \\ v_{gb} \\ v_{gc} \end{bmatrix} = \begin{bmatrix} V_g^N . e^{j(\omega t + \varphi_N)} \\ V_g^N . e^{j(\omega t - \frac{2}{3}\pi + \varphi_N)} \\ V_g^N . e^{j(\omega t + \frac{2}{3}\pi + \varphi_N)} \end{bmatrix} \quad (3)$$

$$\begin{bmatrix} v_{ga}^Z \\ v_{gb}^Z \\ v_{gc}^Z \end{bmatrix} = \frac{1}{3} \begin{bmatrix} 1 & 1 & 1 \\ 1 & 1 & 1 \\ 1 & 1 & 1 \end{bmatrix} . \begin{bmatrix} v_{ga} \\ v_{gb} \\ v_{gc} \end{bmatrix} = \begin{bmatrix} V_g^Z . e^{j(\omega t + \varphi_Z)} \\ V_g^Z . e^{j(\omega t + \varphi_Z)} \\ V_g^Z . e^{j(\omega t + \varphi_Z)} \end{bmatrix} \quad (4)$$

The development of the real parts of the previous equations allows expressing the instantaneous expressions of the sequences P, N, and Z:

$$\begin{bmatrix} v_{ga}^P(t) \\ v_{gb}^P(t) \\ v_{gc}^P(t) \end{bmatrix} = \frac{1}{3} \begin{bmatrix} (V_a + V_b + V_c). \cos(\theta) \\ (V_a + V_b + V_c). \cos(\theta - \frac{2\pi}{3}) \\ (V_a + V_b + V_c). \cos(\theta + \frac{2\pi}{3}) \end{bmatrix} \quad (5)$$

$$\begin{bmatrix} v_{ga}^N(t) \\ v_{gb}^N(t) \\ v_{gc}^N(t) \end{bmatrix} = \frac{1}{3} \begin{bmatrix} (V_a \cos(\theta) + V_b \cos(\theta + \frac{2\pi}{3}) + V_c \cos(\theta - \frac{2\pi}{3})) \\ (V_a \cos(\theta + \frac{2\pi}{3}) + V_b \cos(\theta - \frac{2\pi}{3}) + V_c \cos(\theta)). \\ (V_a \cos(\theta - \frac{2\pi}{3}) + V_b \cos(\theta) + V_c \cos(\theta + \frac{2\pi}{3})) \end{bmatrix} \quad (6)$$

$$\begin{bmatrix} v_{ga}^Z(t) \\ v_{gb}^Z(t) \\ v_{gc}^Z(t) \end{bmatrix} = \frac{1}{3} \begin{bmatrix} (V_a \cos(\theta) + V_b \cos(\theta + \frac{2\pi}{3}) + V_c \cos(\theta - \frac{2\pi}{3})) \\ (V_a \cos(\theta) + V_b \cos(\theta + \frac{2\pi}{3}) + V_c \cos(\theta - \frac{2\pi}{3})) \\ (V_a \cos(\theta) + V_b \cos(\theta + \frac{2\pi}{3}) + V_c \cos(\theta - \frac{2\pi}{3})) \end{bmatrix} \quad (7)$$

The previous complex quantities are difficult to be controlled in the unbalanced mode. We intend to transform them into the synchronous reference frame (SRF) according to Eq. 8. Here, the application of the Park transformation to the real parts of the positive-, negative- and zero-sequences allows establishing their *dqo* components according to the SRF.
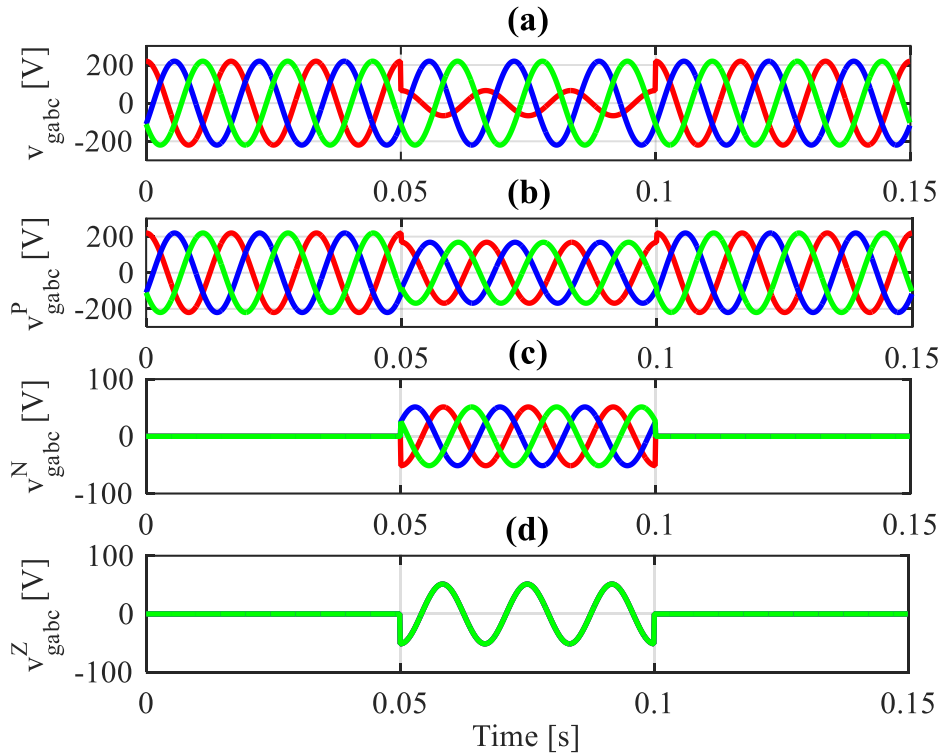

(a)

(b)

(c)

(d)

Fig. 2: Symmetrical sequences systems: (a) Positive sequence, (b) Negative sequence, and (c) Zero sequence

$$\begin{bmatrix} v_d(t) \\ v_q(t) \\ v_0(t) \end{bmatrix} = \frac{1}{2} \sqrt{\frac{2}{3}} \begin{bmatrix} \sum_i V_i + \sum_i V_i \cos(2\theta + 2(i-1)\frac{\pi}{3})) \\ -(\sum_i V_i \sin(2\theta + 2(i-1)\frac{\pi}{3})) \\ \sqrt{2}(\sum_i V_i \sin(\theta + 2(i-1)\frac{\pi}{3})) \end{bmatrix} \text{ i= (a,b,c)} \quad (8)$$

Based on Eq. 8, the simulations elaborated in Fig. 3 show the temporal evolutions of the Park components in the rotating synchronous reference frame during the same scenario in Fig. 2. It is clear that these components, which are constant during the balanced conditions, are oscillating at the double

frequency of the network during the unbalanced state.

To identify fluctuations that arise in *d, q* unbalanced voltage system components, these latest were established according to two references and two Park matrices: The positive synchronous reference frame (PSRF) and the negative synchronous reference frame (NSRF) (Abbassi et al., 2019). The PSRF rotates counterclockwise at a pulsation of $+\omega_s$ and the NSRF rotates clockwise at $-\omega_s$. The transformations have been ensured by the following matrices:

$$[P(+\theta)]_{PSRF} =$$
$$\sqrt{\frac{2}{3}} \begin{bmatrix} \cos(\theta) & \cos(\theta - \frac{2\pi}{3}) & \cos(\theta + \frac{2\pi}{3}) \\ -\sin(\theta) & -\sin(\theta - \frac{2\pi}{3}) & -\sin(\theta + \frac{2\pi}{3}) \\ \frac{1}{\sqrt{2}} & \frac{1}{\sqrt{2}} & \frac{1}{\sqrt{2}} \end{bmatrix} \quad (9)$$

$$[P(-\theta)]_{NSRF} = \sqrt{\frac{2}{3}} \begin{bmatrix} \cos(\theta) & \cos(\theta + \frac{2\pi}{3}) & \cos(\theta - \frac{2\pi}{3}) \\ \sin(\theta) & \sin(\theta + \frac{2\pi}{3}) & \sin(\theta - \frac{2\pi}{3}) \\ \frac{1}{\sqrt{2}} & \frac{1}{\sqrt{2}} & \frac{1}{\sqrt{2}} \end{bmatrix}$$
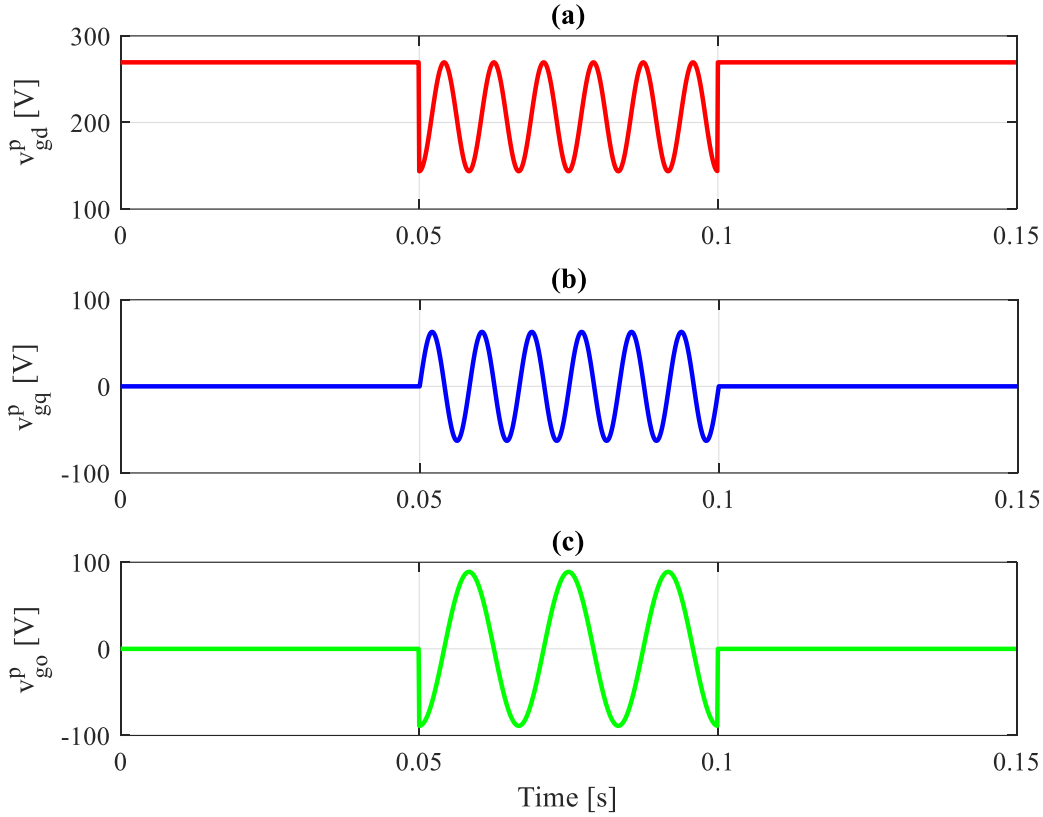$$(10)$$

Fig. 3: Components of the grid voltages system in the SRF: (a) d, (b) q, and (c) o

The fluctuations that occur during the grid voltage imbalance are quantified (Zhang et al., 2021). The unbalanced d and q components in PSRF stay as the totality of the constant d and q components of the positive sequence in PSRF and the same components of the negative sequence in PSRF which show oscillations at twice the times of the grid frequency as shown in 11 and 12 (Abbassi et al., 2013).

$$v_{gd}^{p} = v_{gd}^{Pp} + v_{gd}^{Np} = v_{gd}^{Pp} + v_{gd}^{Nn} e^{-j2\theta} \quad (11)$$
$$v_{gq}^{p} = v_{gq}^{Pp} + v_{gq}^{Np} = v_{gq}^{Pp} + v_{gq}^{Nn} e^{-j2\theta} \quad (12)$$

In the same context, the unbalanced d and q components in NSRF are the sum of the constant d and q components of the negative sequence in NSRF and the same components of the positive sequence in NSRF which are oscillating 13 and 14 (Abbassi et al., 2019).

$$v_{gd}^{n} = v_{gd}^{Nn} + v_{gd}^{Pn} = v_{gd}^{Nn} + v_{gd}^{Pp} e^{+j2\theta} \quad (13)$$
$$v_{gq}^{n} = v_{gq}^{Nn} + v_{gq}^{Pn} = v_{gq}^{Nn} + v_{gq}^{Pp} e^{+j2\theta} \quad (14)$$

The DPGS performs when it is connected to a balanced grid. Once a grid fault occurs, there cannot be a guarantee of the same type of performance in the DPGS. Hence an effective control algorithm is to be established to secure the connection of a DPGS to the grid even in case of disturbances that may occur.

2.3. Problem statements

In utmost cases, the converter at the grid side represented as GSC is likely impacted by momentary disturbances and disruptions that could pass over the electric system (Abbassi et al., 2019). Particularly, asymmetrical grid voltage imbalances can affect the generators.

According to conventional solutions, it is advisable to disconnect the DPGS from the unbalanced network to prevent unwanted effects from spreading to the production units through the GSC. Indeed, the voltage imbalance generates severe fluctuations at the level of the active and reactive powers and also at the level of the DC bus voltage (Abbassi et al., 2019; Zhang et al., 2021). These oscillations at double the frequency of the network come mainly from fluctuations in the Park components of currents and voltages. The major problem here is that the inner loop regulators and the outer loop regulators that handle currents and voltages, respectively, will operate under poor conditions which are due to the occurrence of the negative and zero sequences.

3. Proposed control approach for the GSC under unbalanced conditions

At the PCC, negative sequence voltage causes asymmetrical faults and eventually causes a wave of DC bus voltage. The oscillations in the system occur double the time due to the power injected into the network (Mahlooji et al., 2018). Hence, the power generation should consider the safety of the network, synchronization, and operation before connecting to a network.

In the following, a comparative study is made between two GSC control strategies to assess their performance during grid imbalance conditions (Chen et al., 2016). By referring to the BS-EN-50160 standard, the aim is to provide, with the proper control of the GSC, "fictitious" isolation between the faulty network and the DPGS to prevent the harmful effects of the fault on the network side propagate to production units during fault phases. The block diagram of the proposed control strategy for the control of a three-phase four-leg inverter is shown in Fig. 4.
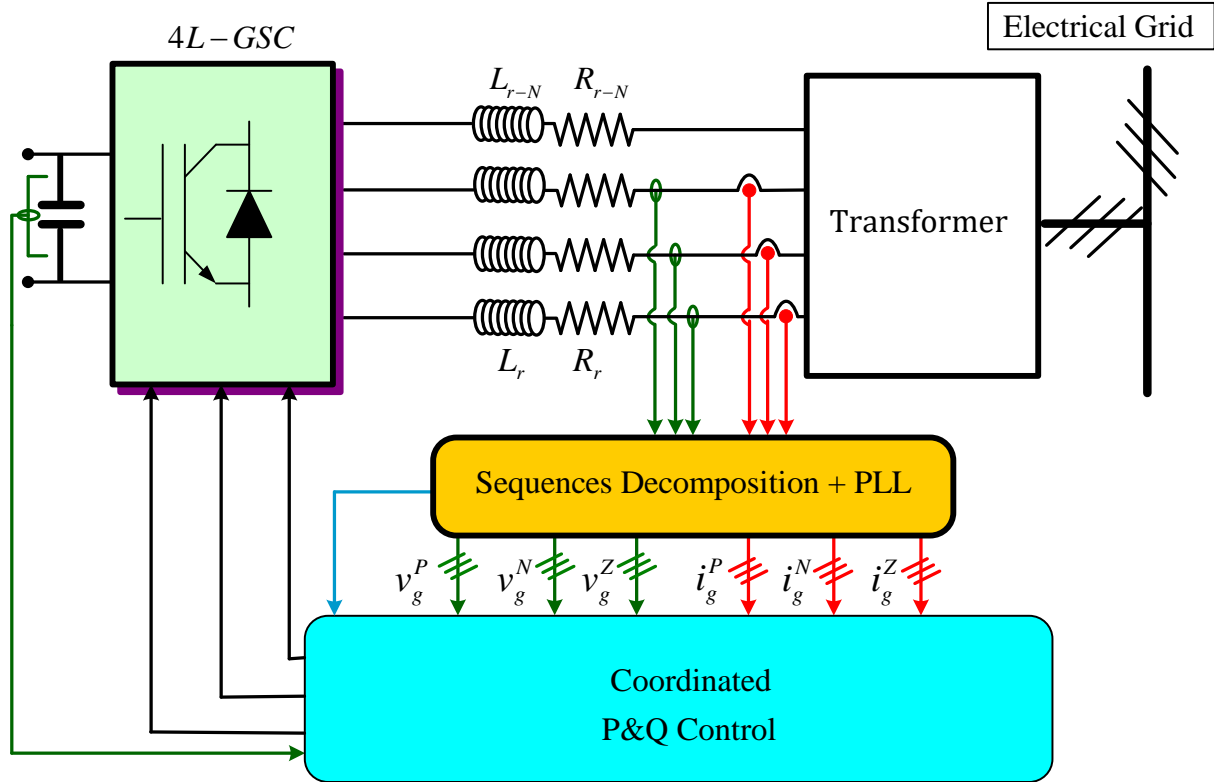

Fig. 4: Block diagram of the proposed control strategy

The proposed method is based on Fortescue's theory (Abbassi et al., 2019) which allows the extraction of symmetrical sequences of complex systems of voltages (or currents) according to Eqs. 2, 3, and 4. Herein, the complex grid voltage system is established through the phasor writing approach (Abbassi et al., 2012) as in 15.

$$
\begin{aligned}
v_{ga}(t) &= V_a[\cos(\omega t + \varphi_a) + j\sin(\omega t + \varphi_a)] = V_a e^{j(\omega t + \varphi_a)} \\
v_{gb}(t) &= V_b\left[\cos\left(\omega t - \frac{2\pi}{3} + \varphi_b\right) + j\sin\left(\omega t - \frac{2\pi}{3} + \varphi_b\right)\right] = \\
&\quad V_b e^{j\left(\omega t - \frac{2\pi}{3} + \varphi_b\right)} \\
v_{gc}(t) &= V_c\left[\cos\left(\omega t + \frac{2\pi}{3} + \varphi_c\right) + j\sin\left(\omega t + \frac{2\pi}{3} + \varphi_c\right)\right] = \\
&\quad V_c e^{j\left(\omega t + \frac{2\pi}{3} + \varphi_c\right)}
\end{aligned}
\tag{15}
$$

Based on the obtained symmetrical sequences of Eqs. 5, 6, and 7 After applying Fortescue conversion, the sequences the components, v_{gabc}^P, v_{gabc}^N, and v_{gabc}^Z are achieved. The zero elements fluctuate at the grid frequency. Due to this, there should be further transformation which will provide the voltage vector of the zero-sequence a balance to the

system which has a 120° shift in phase with identical amplitudes. The investigation is established for the positive and the negative frames (Abbassi et al., 2019). Their rotation clockwise and anticlockwise are represented as $+\omega_s$ and $-\omega_s$.

In the synchronous frames, the voltage, and current of all the three sequences are deprived of the component which fluctuates and is regulated through the PI control loop which improves the accuracy of the algorithm (Fig. 5).

4. Results and discussion

The first simulation is focused on the evaluation of the impact of the voltage imbalance on the power system in the case of a classical control system. The voltage dip occurs at 2.05 seconds in phase "a" with 50% of its amplitude. Fig. 6 depicts the voltages of the grid during the over mentioned conditions. The negative effects of such imbalance on the DC link voltage and grid currents in terms of oscillations at twice the frequency (2.ω) and distortions (Fig. 7), respectively.
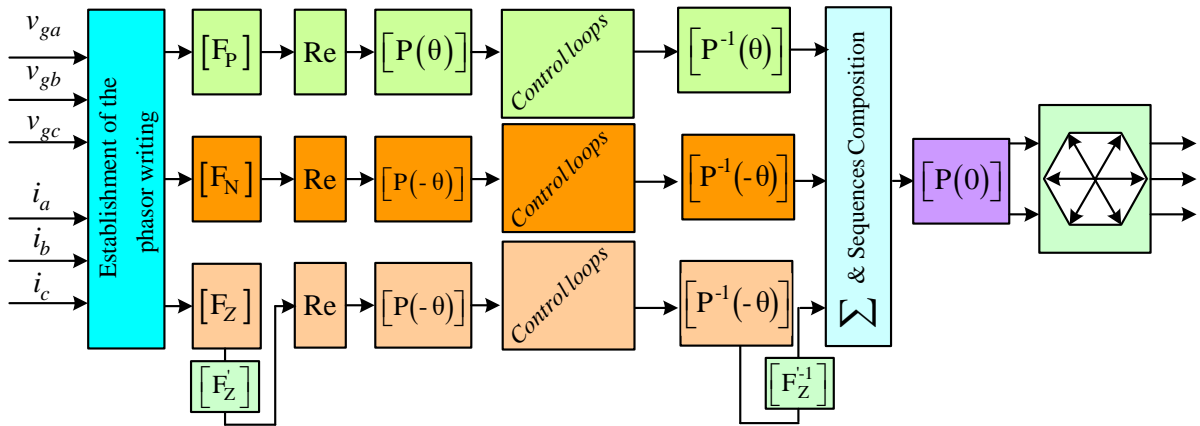
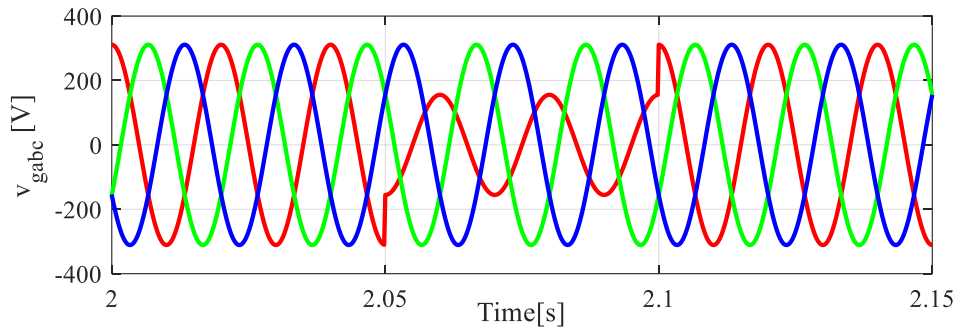**Fig. 5:** Transformations and control loops of the proposed control strategy

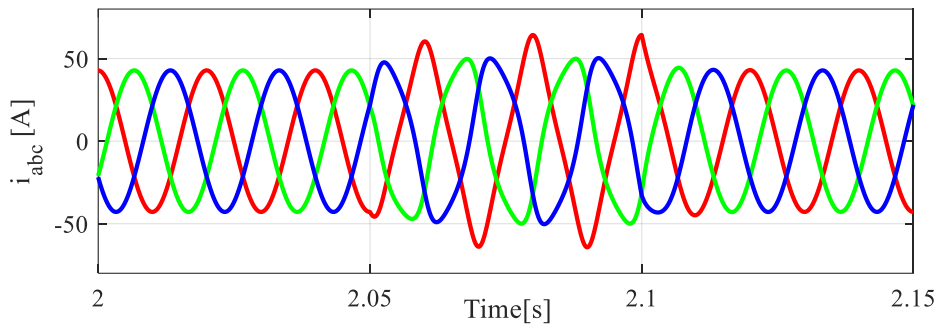
Fig. 6: Unbalanced grid voltages

Fig. 7: Distorted grid currents

Under the same conditions, the active and reactive powers on the network side, which are perfectly constant in a balanced regime, show the occurrence of oscillations during the studied voltage fault. According to Fig. 8, the oscillations of the two powers are also at the frequency 2.ω.
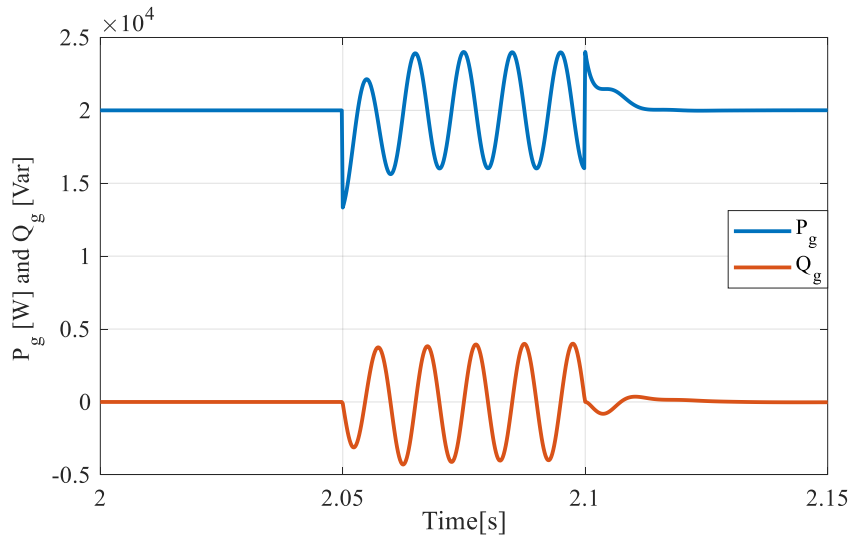

Fig. 8: Quality of exchanged powers

Figs. 7 and 8 illustrated the performance of the ICPS control strategy (Abbassi et al., 2019). In order to validate the proposed control and to test the performances it can show in front of a voltage unbalance, our attention has been focused on the ability of this control to overcome the harmful effects of the unbalance occurrence compared to the ICPS control technique. Indeed, under the same conditions as in Fig. 6, the currents delivered to the network keep their sinusoidal nature without distortions (Fig. 9).
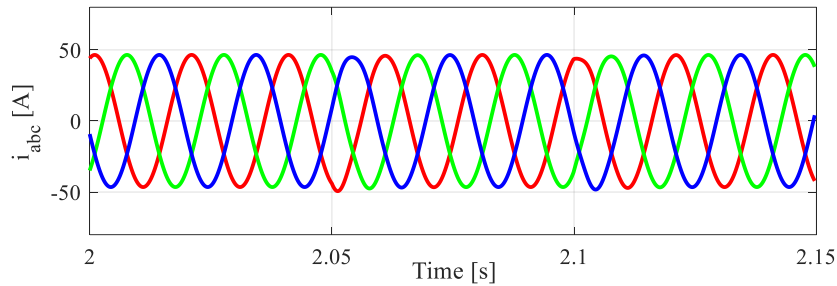

Fig. 9: Balanced generated grid currents

Only the current amplitude of the faulty phase shows a negligible decrease which is quickly canceled out. The transient regime, which is without influence, is also difficult to be observed on the power curves P_g and Q_g (Fig. 10).
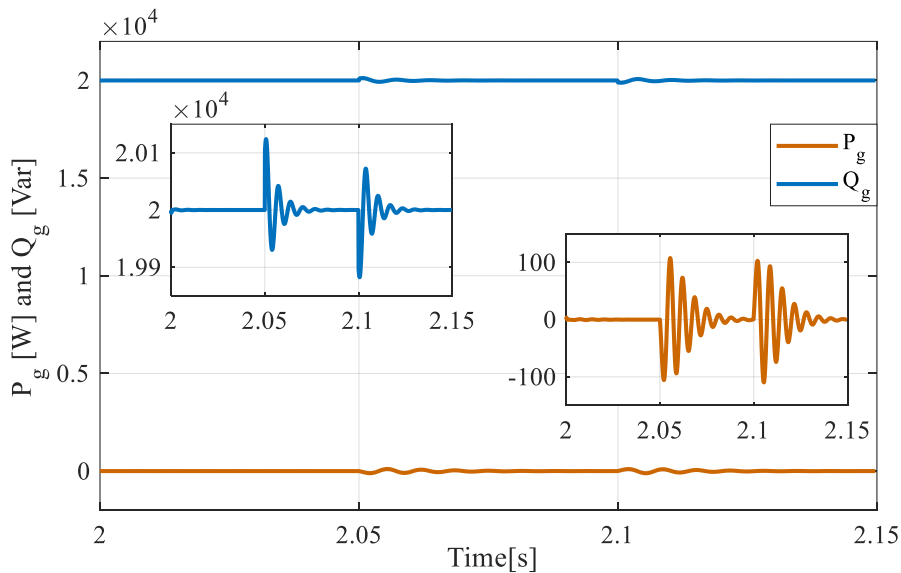

Fig. 10: Controlled active and reactive powers

Contrary to scenario 1 reserved for the classical control, the powers P_g and Q_g generated by the proposed control undergo very negligible oscillations during the application and the disappearance of the voltage fault and which are quickly canceled out. The active power peaks do not exceed 120W while those in Fig. 8 reach 4500W.

The results of the simulations show clearly that the proposed control is very effective during voltage imbalances of the electrical network.

5. Conclusion

This paper was interested in the study of a three-phase inverter connected to the grid in the presence of unbalanced voltages. A control system based on the theory of symmetrical components and the control of electrical quantities in two different rotating reference frames was very effective when applied to a three-phase four-leg VSI converter. Indeed, in comparison with a classical control, the results found showed a significant reduction of the DC voltage ripple and the oscillations at twice the fundamental frequency of the electrical quantities exchanged with the grid even in case of voltage unbalance.

Compliance with ethical standards

Conflict of interest

The author(s) declared no potential conflicts of interest with respect to the research, authorship, and/or publication of this article.

References

Abbassi R, Boudjemline A, Abbassi A, Torchani A, Gasmi H, and Guesmi T (2018). A numerical-analytical hybrid approach for the identification of SDM solar cell unknown parameters. Engineering Technology and Applied Science Research, 8(3): 2907-2913. https://doi.org/10.48084/etasr.2027

Abbassi R, Hammami M, and Chebbi S (2013). Improvement of the integration of a grid-connected wind-photovoltaic hybrid system. In the International Conference on Electrical Engineering and Software Applications, IEEE, Hammamet, Tunisia: 1-5. https://doi.org/10.1109/ICEESA.2013.6578357

Abbassi R, Marrouchi S, Hessine MB, Chebbi S, and Jouini H (2012). Voltage control strategy of an electrical network by the integration of the UPFC compensator. International Review on Modelling and Simulations, 5(1): 380-384.

Abbassi R, Marrouchi S, Saidi S, Abbassi A, and Chebbi S (2019). Optimal energy management strategy and novel control approach for DPGSs under unbalanced grid faults. Journal of Circuits, Systems and Computers, 28(4): 1950-1957. https://doi.org/10.1142/S0218126619500579

Aboagye B, Gyamfi S, Ofosu EA, and Djordjevic S (2022). Investigation into the impacts of design, installation, operation and maintenance issues on performance and degradation of installed solar photovoltaic (PV) systems. Energy for Sustainable Development, 66: 165-176. https://doi.org/10.1016/j.esd.2021.12.003

Bensalem Y, Abbassi R, and Jerbi H (2021). Fuzzy logic based-active fault tolerant control of speed sensor failure for five-phase PMSM. Journal of Electrical Engineering and Technology, 16: 287-299. https://doi.org/10.1007/s42835-020-00559-7

Chen HC, Lee CT, Cheng PT, Teodorescu R, and Blaabjerg F (2016). A low-voltage ride-through technique for grid-connected converters with reduced power transistors stress. IEEE Transactions on Power Electronics, 31(12): 8562-8571. https://doi.org/10.1109/TPEL.2016.2522511

Hamidi F, Olteanu SC, Popescu D, Jerbi H, Dincă I, Ben Aoun S, and Abbassi R (2020). Model based optimisation algorithm for maximum power point tracking in photovoltaic panels. Energies, 13(18): 4798. https://doi.org/10.3390/en13184798

Han Y, Li H, Shen P, Coelho EAA, and Guerrero JM (2016). Review of active and reactive power sharing strategies in hierarchical controlled microgrids. IEEE Transactions on Power Electronics, 32(3): 2427-2451. https://doi.org/10.1109/TPEL.2016.2569597

Hassan TU, Abbassi R, Jerbi H, Mehmood K, Tahir MF, Cheema KM, and Khan IA (2020). A novel algorithm for MPPT of an isolated PV system using push pull converter with fuzzy logic controller. Energies, 13(15): 4007. https://doi.org/10.3390/en13154007

Jin J, Zhang X, Xu L, Wen Q, and Guo X (2021). Impacts of carbon trading and wind power integration on carbon emission in the power dispatching process. Energy Reports, 7: 3887-3897. https://doi.org/10.1016/j.egyr.2021.06.077

Latifi M, Abbassi R, Jerbi H, and Ohshima K (2021). Improved krill herd algorithm based sliding mode MPPT controller for variable step size P&O method in PV system under simultaneous change of irradiance and temperature. Journal of the Franklin Institute, 358(7): 3491-3511. https://doi.org/10.1016/j.jfranklin.2021.02.021

Li N, Su Z, Jerbi H, Abbassi R, Latifi M, and Furukawa N (2021). Energy management and optimized operation of renewable sources and electric vehicles based on microgrid using hybrid gravitational search and pattern search algorithm. Sustainable Cities and Society, 75: 103279. https://doi.org/10.1016/j.scs.2021.103279

Mahlooji MH, Mohammadi HR, and Rahimi M (2018). A review on modeling and control of grid-connected photovoltaic inverters with LCL filter. Renewable and Sustainable Energy Reviews, 81: 563-578. https://doi.org/10.1016/j.rser.2017.08.002

Maisanam AKS, Biswas A, and Sharma KK (2021). Integrated socio-environmental and techno-economic factors for designing and sizing of a sustainable hybrid renewable energy system. Energy Conversion and Management, 247: 114709. https://doi.org/10.1016/j.enconman.2021.114709

Mohammadinodoushan M, Abbassi R, Jerbi H, Ahmed FW, and Rezvani A (2021). A new MPPT design using variable step size perturb and observe method for PV system under partially shaded conditions by modified shuffled frog leaping algorithm-SMC controller. Sustainable Energy Technologies and Assessments, 45: 101056. https://doi.org/10.1016/j.seta.2021.101056

Nasr A, Gu C, Wang X, Buticchi G, Bozhko S, and Gerada C (2022). Torque-performance improvement for direct torque-controlled PMSM drives based on duty-ratio regulation. IEEE Transactions on Power Electronics, 37(1): 749-760. https://doi.org/10.1109/TPEL.2021.3093344

Oliva S, Muñoz J, Fredes F, and Sauma E (2022). Impact of increasing transmission capacity for a massive integration of renewable energy on the energy and environmental value of distributed generation. Renewable Energy, 183, 524-534. https://doi.org/10.1016/j.renene.2021.11.025

Saidi S, Abbassi R, and Chebbi S (2014). Virtual flux based direct power control of shunt active filter. Scientia Iranica, 21(6): 2165-2176.

Saidi S, Abbassi R, and Chebbi S (2016). Quality improvement of shunt active power filter with direct instantaneous power estimator based on virtual flux. International Journal of Control, Automation and Systems, 14(5): 1309-1321. https://doi.org/10.1007/s12555-014-0264-4

Tang S, Jiang M, Abbassi R, and Jerbi H (2021). A cost-oriented resource scheduling of a solar-powered microgrid by using the hybrid crow and pattern search algorithm. Journal of Cleaner Production, 313: 127853. https://doi.org/10.1016/j.jclepro.2021.127853

Venkatesan M, Adhavan B, Suresh K, Balachander K, and Prabakar MLC (2020). Research on FPGA controlled three phase PV inverter using multi carrier PWM control schemes. Microprocessors and Microsystems, 76: 103089. https://doi.org/10.1016/j.micpro.2020.103089

Wang X, Wang Z, Xu Z, Cheng M, and Hu Y (2020). Optimization of torque tracking performance for direct-torque-controlled PMSM drives with composite torque regulator. IEEE Transactions on Industrial Electronics, 67(12): 10095-10108. https://doi.org/10.1109/TIE.2019.2962451

Yin N, Abbassi R, Jerbi H, Rezvani A, and Müller M (2021). A day-ahead joint energy management and battery sizing framework based on θ-modified krill herd algorithm for a renewable energy-integrated microgrid. Journal of Cleaner Production, 282: 124435. https://doi.org/10.1016/j.jclepro.2020.124435

Zamani MH, Riahy GH, and Abedi M (2015). Rotor-speed stability improvement of dual stator-winding induction generator-based wind farms by control-windings voltage oriented control. IEEE Transactions on Power Electronics, 31(8): 5538-5546. https://doi.org/10.1109/TPEL.2015.2495256

Zhang C, Isobe T, Suul JA, Dragičević T, and Molinas M (2021). Parametric stability assessment of single-phase grid-tied VSCs using peak and average dc voltage control. IEEE Transactions on Industrial Electronics, 69(3): 2904-2915. https://doi.org/10.1109/TIE.2021.3068551

Zhao L, Jerbi H, Abbassi R, Liu B, Latifi M, and Nakamura H (2021). Sizing renewable energy systems with energy storage systems based microgrids for cost minimization using hybrid shuffled frog-leaping and pattern search algorithm. Sustainable Cities and Society, 73: 103124. https://doi.org/10.1016/j.scs.2021.103124